Journal of the Korea Concrete Institute
Vol.17 No.5, pp.835~842, October, 2005

Bond-Strengthening Hooks for RC Members with High Strength Spirals

Kil-Hee Kim[1)*] and Yuichi Sato[2)]

[1)]*Dept. of Architectural Engineering, Kongju National University, 314~701, Korea*
[2)]*Dept. of Urban Environment Engineering, Kyoto University, Japan*

(Received February 24, 2005, Accepted August 30, 2005)

Abstract

This paper presents an experimental investigation of bond-strengthening hooks as a new method to increase bond strength along flexural reinforcing bars in reinforced concrete (RC) beams and columns. The RC members, which consisted of 1,300 MPa-class spirals as shear reinforcement, often suffered from bond splitting failure. The proposed method attempts to increase confining stiffness around the flexural bars by placing U-shaped hooks and to prevent premature bond splitting failure. Twelve specimens with varied amounts and sizes of the hooks were prepared to verify the strengthening effectiveness under monotonic and cyclic loading conditions. The test result indicated that the hooks increased the bond strength along the flexural bars although the strengthening effectiveness was limited by effective reinforcement ratio p_{be}. This limit is determined by size of stress-transmitting zones of concrete around anchors of the hooks. Anchors of the hooks are recommended to be longer than twelve times the hook diameter and inserted deeper than a quarter of the member depth ($D/4$). Proposed design equations provide modest estimates of the shear strengths.

Keywords: beam, column, shear strength, bond strength, hook, high strength spirals

1. Introduction

Ultra high strength spiral provides large shear capacity to a RC member without congestion due to over-reinforce-ment. The spirals are especially effective for members of high-rise RC buildings where large flexural and shear capacities are required. Reduction of amount of shear reinforcement, however, often accompanies with reduction of bond strength along flexural reinforcing bars. Fig. 1 compares two column specimens in a previous work[1)]; Specimen K1 consisted of a 1,300 MPa-class spiral while K2 was reinforced with larger amount of normal strength ties. Specimens K1 and K2 possessed an equivalent shear reinforcement level in term of $p_w\sigma_{wy}$ by 7.4 MPa to 7.8 MPa, where p_w = shear reinforcement ratio, and σ_{wy} = yield stress of shear reinforcing bar. Nevertheless, specimen K1 resulted in a remarkably inferior ductility in comparison with K2.

The deterioration of specimen K1 was caused by bond splitting failure along the flexural bars as crack pattern in Fig. 1. The comparison between specimens K1 and K2 indicates that the bond strength along the flexural bars depends on rather stiffness of the lateral reinforcement than the reinforcement's strength.

According to AIJ(Architectural Institute of Japan) Guidelines[3)], the shear strength V_u is given by Eqs. (1)~(10).

$$V_u = \min(V_{u1}, V_{u2}, V_{u3}, V_{bu}) \tag{1}$$

$$V_{u1} = p_w \sigma_{wy} b_e j_e \cot\phi + \left(\nu\sigma_B - \frac{5p_w\sigma_{wy}}{\lambda}\right)\frac{bD}{2}\tan\theta \tag{2}$$

$$V_{u2} = \frac{\lambda\nu\sigma_B + p_w\sigma_{wy}}{3} b_e j_e \tag{3}$$

$$V_{u3} = \frac{\lambda\nu\sigma_B}{2} b_e j_e \tag{4}$$

$$V_{bu} = j_e \tau_{bu} \Sigma\psi + \left(\nu\sigma_B - \frac{2.5\tau_{bu}\Sigma\psi}{\lambda b_e}\right)\frac{bD}{2}\tan\theta \tag{5}$$

Where,

$$p_w = \pi N_w d_{bw}^2 / (4\, b_e\, s_w) \tag{6}$$

* *Corresponding author*
Email address: kimkh@kongju.ac.kr

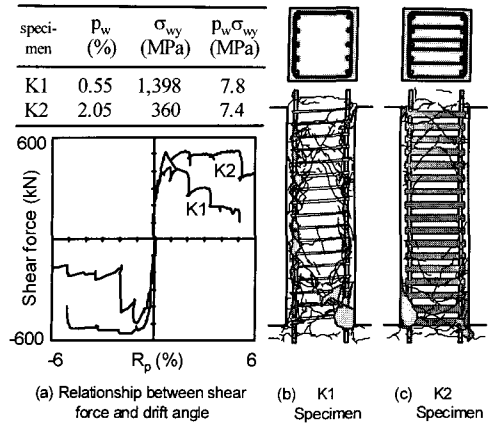

Fig. 1 Specimens with and without bond splitting failure

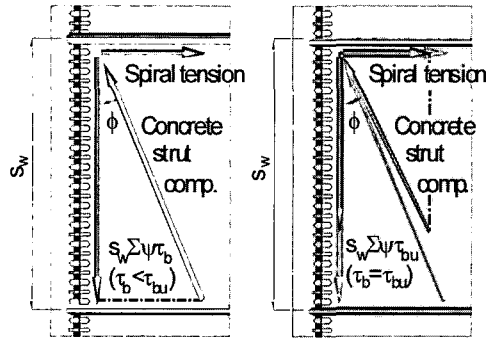

(a) Equilibrium in Eqs.(2)-(4) (b) Equilibrium in Eq.(5)

Fig. 2 Limit of stress-transmission due to bond strength reduction

$$\cot\phi = 2 - 20\,R_p \tag{7}$$

ν = effective concrete strength factor

$$= (1 - 20\,R_p)\,(0.7 - \sigma_B / 200) \tag{8}$$

$$\tan\theta = \sqrt{(L/D)^2 + 1} - L/D \tag{9}$$

λ = effective area factor for truss action

$$= 1 - s_w / (2\,j_e) - b_s / (4\,j_e) \tag{10}$$

b = width of member;
b_e = effective width of member (= width of core concrete encased in shear reinforcing bars; see Tables 1 and 2)
b_s = largest distance between ties
d_{bw} = diameter of shear reinforcing spiral
D = depth of member
j_e = effective depth of member
L = clear span length
N_w = number of flexural bars hooked by spirals
R_p = drift angle of member
s_w = spacing of shear reinforcing spirals
ϕ = angle of concrete truss strut
θ = angle of concrete arch strut
σ_B = compressive concrete strength(MPa)
τ_{bu} = bond strength along flexural bar
$\Sigma\psi$ = total of diameter of flexural bar

Equations (2), (3) and (4) give the strengths determined by amount and strength of shear reinforcement, concrete strength and member geometry. However, a smaller spiral ratio p_w reduces bond strength along the longitudinal bar τ_{bu}. The reduction of the τ_{bu} results in a smaller tensile force in the spiral and a smaller compressive force in the concrete strut as illustrated in Fig. 2.

Equation (5) defines a shear strength limited by the bond strength τ_{bu}. The τ_{bu} is given by Eqs. (11)~ (19).

$$\tau_{bu} = \beta_p\,\alpha_t\,(\tau_c + \tau_s) \tag{11}$$

$$\beta_p = 1 - 10\,R_p \tag{12}$$

$$\alpha_t = 0.75 + \sigma_B / 400 \quad \text{for top bar in a beam}$$
$$= 1 \quad \text{for others} \tag{13}$$

$$\tau_c = (0.085\,b_i + 0.1)\sqrt{\sigma_B} \tag{14}$$

$$\tau_s = (54 + 45\,N_w / N_t)\,(b_{si} + 1)\,p_w \quad \text{for } b_{si} < b_{ci} \tag{15}$$

$$= 36.5\,\pi\,d_{bw}^2 / (s_w\,d_{bt}) \quad \text{for } b_{si} > b_{ci} \tag{16}$$

$$b_i = \min(b_{si},\, b_{ci}) \tag{17}$$

b_{si} = coefficient for side splitting mode

$$= b / (N_t\,d_{bt}) - 1 \tag{18}$$

b_{ci} = coefficient for corner splitting mode

$$= \sqrt{2}\,(d_{cw} + d_{cd} - d_{bt}) / d_{bt} - 1 \tag{19}$$

where,
d_{bt} = diameter of flexural bar
d_{cd} = thickness of cover in depth direction
d_{cw} = thickness of cover in width direction and
N_t = number of flexural bars in a layer

The Guidelines adopt an assumption that the τ_{bu} comprises contribution of concrete τ_c and contribution of steel τ_s. The latter is further classified into two cases according to the bond failure modes. The coefficient b_i defined in Eq. (17) represents the failure mode, which is the smaller between b_{si} given by Eq. (18) and b_{ci} by Eq. (19). The side splitting mode ($b_{si} < b_{ci}$) is usually a case in a member with heavy flexural reinforcement, where adjacent longitudinal bars are arranged with small spacing.

Equation (15) gives steel contribution to the τ_{bu} in the case of side splitting mode. It takes account of the effectiveness of the shear reinforcement by the cross-sectional area ratio p_w, not by the $p_w\sigma_{wy}$ term.

Fig. 3 illustrates application of U-shaped hook as one of the possible methods to increase the bond strength, which saves cost and labor[5]. The hooks can be applied after completion of arrangement of flexural and shear reinforcements.

In addition, the hooks are made of inexpensive normal strength steel and can be easily formed into the shape. The bond-strengthening method proposed herein will therefore achieve increase of shear and bond capacities at a lower cost, avoiding a congested bar arrangement.

This paper presents an experimental study to verify effectiveness of the bond-strengthening hooks with varied amounts and shapes. The test results showed that the hooks increased the bond strength and kept the RC beams and columns from premature shear failure under monotonic and even cyclic loading conditions.

Through the test, this paper discusses the influences of the amounts and the shapes of the hooks on the bond strength τ_{bu}. The effective concrete strength factor ν will be defined as a function of only concrete strength σ_B[3] although the actual strength is influenced by the reinforcement[1].

2. Experimental program

Twelve specimens were prepared, which consisted of 1,300 MPa-class spirals as shear reinforcement. Eight of them belonged to N series(Table 1), while the rest to H series(Table 2). Fig. 4 illustrates geometries of the specimens and Fig. 5 illustrates test apparatus. Strains in the reinforcements were measured with strain gauges (SG). Table 3 shows the material properties.

The N series represented beams with relatively light shear reinforcement (p_w = 0.29 %) and normal concrete strength (σ_B = 35.7 MPa). The specimens had span length of 900mm, 300 mm deep and 300 mm wide. The shear span to depth ratio a/D was 1.5. The flexural reinforcement consisted of twelve steel bars with diameter of 16 mm.

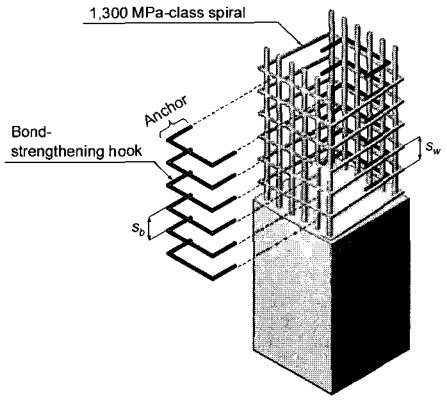

Fig. 3 Bond-strengthening hook

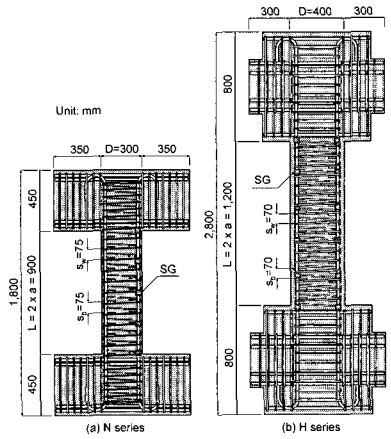

Fig. 4 Specimens

The H series represented columns at lower stories of high-rise RC buildings. The specimens therefore consisted of heavier shear reinforcement (p_w = 0.55 %) and concrete with higher strength (σ_B = 45.1 MPa).

Table 1 Cross-sections of N series specimens

Specimen	H0	H4	H8	H6C
Cross-Section (unit : mm)	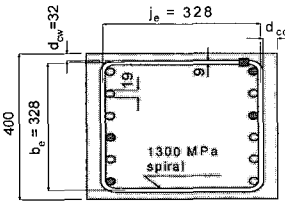	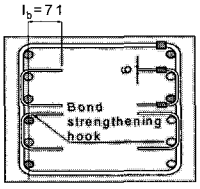	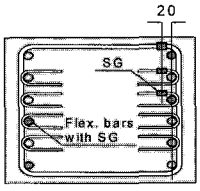	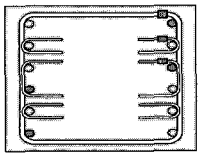
	N_b=0, N_{bh}=0	N_b=4, N_{bh}=2	N_b=8, N_{bh}=1	N_b=6, N_{bh}=2

Table 2 Cross-sections of H series specimens

Specimen	N1	N2 and N7	N3 and N8	N4	N5	N6
Cross-Section (unit : mm)	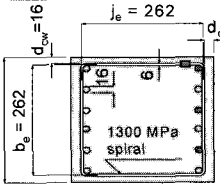	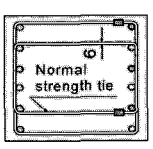	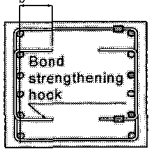	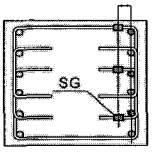	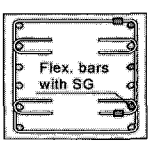	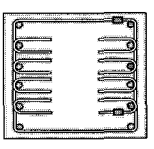
	N_b=0, N_{bh}=0	N_b=0, N_{bh}=0	N_b=2, N_{bh}=4	N_b=4, N_{bh}=3	N_b=4, N_{bh}=1	N_b=8, N_{bh}=1

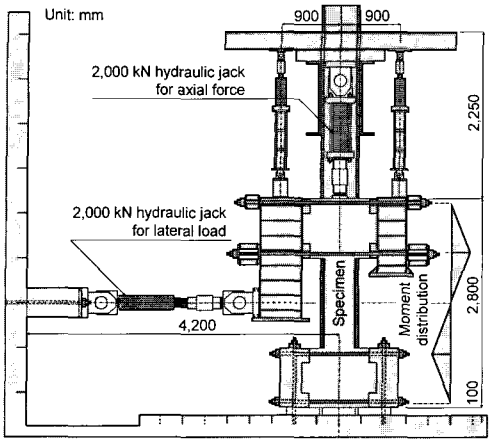

Fig. 5 Test set-up (H series)

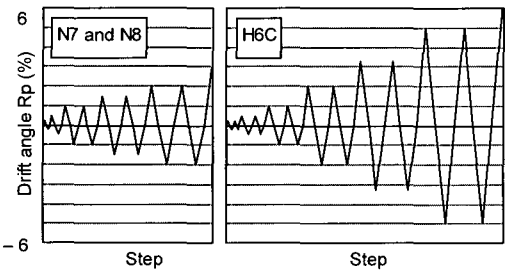

(a) N Series (b) H Series

Fig. 6 Cycle load patterns

The span, depth and width are enlarged up to 1200 mm, 400 mm and 400 mm, respectively. The a/D and axial force ratio $N / (bD\sigma_B)$ are respectively 1.5 and 0.15. Twelve bars with diameter of 19 mm were provided as flexural reinforcement. Specimens N1, N2, N3, N4, N5, N6, H0, H4 and H8 were subjected to monotonic loads. These specimens consisted of flexural bars with yield stress around 850 MPa in an attempt to induce shear failure before flexural yielding. The specimens contain varied numbers and widths of the bond-strengthening hooks made of normal strength steel with diameter of 6 mm. The N_b is defined as the total of anchors of the hooks (Fig. 3) in a side of a specimen. The N_{bh} is number of the flexural bars contacting with a hook, and indirectly indicates the width of the hook. The anchor length l_b, which is distance between centroid of the flexural bar and end of the anchor, was determined according to two requirements by the AIJ. Firstly, Recommendation for Detailing and Placing of Concrete Reinforcement[2] requires twelve times the bar diameter as the anchor length. Secondly, the Inelastic Displacement Concept Guidelines[3] require bond strengthening along flexural bars in a zone within $D/4$–deep from the member surface. The l_b was thus determined around 70 mm. Equation (20) gives cross-sectional area ratio of the hooks p_b.

Table 3 Material properties

Specimen	N1~N6	N7, N8	H0~H8	H6C
σ_B (MPa)	35.7	35.7	45.1	45.1
ε_c (*10-3)	---	---	2.76	2.76
σ_{ty} (MPa)	837	360	860	400
σ_{tu} (MPa)	916	499	966	588
E_{st} (GPa)	183	179	157	159
σ_{wy} (MPa)	1,387	1,387	1,398	1,398
σ_{wu} (MPa)	1,391	1,391	1,481	1,481
E_{sw} (GPa)	181	181	194	194
σ_{by} (MPa)	305	305	409	409
σ_{bu} (MPa)	452	452	500	500
E_{sb} (GPa)	185	185	168	168

σ_B : Compressive strength of concrete
ε_c : Strain at compressive strength of concrete
σ_{ty}, σ_{tu} : Respectively yield strength and tensile strength of flexural bar
E_{st} : Modulus of elasticity of flexural bar
σ_{wy}, σ_{wu} : Respectively yield strength and tensile strength of shear reinforcing bar
E_{st} : Modulus of elasticity of shear reinforcing bar
σ_{by}, σ_{bu} : Respectively yield strength and tensile strength of bond strengthening hook
E_{sb} : Modulus of elasticity of bond strengthening hook

$$p_b = \sigma N_b d_{bb}^2 / (4 b_e s_b) \quad (20)$$

where,

d_{bb} = diameter of bond-strengthening hook
s_b = spacing of bond-strengthening hooks.

Specimens N2 and N7 contained no hook, but a set of closed tie made of normal strength steel instead. The N_b and the N_{bh} of N2 and N7 were therefore 0 and 0, respectively.

Specimens N7, N8 and H6C were subjected to cyclic loads. Ratio of shear strength V_u to flexural strength V_y of a member in an actual building is usually larger than 1.0. For this reason, the specimens consisted of flexural bars with lower yield stresses (360 MPa or 400 MPa) in order to reduce V_y. Fig. 6 shows the applied cyclic load patterns.

Table 4 shows the calculated shear strengths of the specimens using Eqs.(1)–(19) and equations presented in the following sections. All of the specimens were designed to satisfy $V_{bu} < \text{Min}(V_{u1}, V_{u2}, V_{u3})$ in order to estimate the bond strength τ_{bu} by inducing the bond splitting failure along the flexural bars. Table 4 also presents the shear strength V_u according to the AIJ's Guidelines, where contributions of the bond-strengthening hooks were neglected.

3. Test results

Table 4 shows the experimental shear strengths V_{exp}. The V_{exp} of specimens with the bond-strengthening hooks under

Table 4 Test result

Specimen		N1	N2	N3	N4	N5	N6
p_b	(%)	0.00	0.00	0.29	0.58	0.58	1.15
p_w (σ_{wy} > 1,300 MPa)	(%)	0.29	0.29	0.29	0.29	0.29	0.29
p_w (σ_{wy} = 305 MPa)	(%)	0.00	0.29	0.00	0.00	0.00	0.00
Min (V_{u1}, V_{u2}, V_{u3})	(kN)	348	452	348	348	348	348
V_{bu}	(kN)	236	290	276	298	298	298
V_u (AIJ Guidelines)	(kN)	236	290	236	236	236	236
V_{exp}	(kN)	545	545	545	545	545	545
V_y	(kN)	299	374	375	433	429	406
Failure mode*		B	B	B	S+B	S+B	S+B
τ_{bu}	(MPa)	2.35	3.24	3.24	3.74	3.74	3.74
τ_{bu} (AIJ Guidelines)	(MPa)	2.35	3.24	2.35	2.35	2.35	2.35
$\tau_{b,exp}$	(MPa)	3.42	4.09	3.99	4.55	4.34	4.63
Specimen		N7	N8	H0	H4	H8	H6C
p_b	(%)	0.00	0.29	0.00	0.49	0.99	0.74
p_w (σ_{wy} > 1,300 MPa)	(%)	0.29	0.29	0.55	0.55	0.55	0.55
p_w (σ_{wy} = 305 MPa)	(%)	0.29	0.00	0.00	0.00	0.00	0.00
Min (V_{u1}, V_{u2}, V_{u3})	(kN)	452	348	709	709	709	709
V_{bu}	(kN)	290	276	472	628	628	628
V_u (AIJ Guidelines)	(kN)	290	236	472	472	472	472
V_{exp}	(kN)	235	235	1087	1087	1087	670
V_y	(kN)	264	268	599	742	819	625
Failure mode*		F	F	B	B	B	F+S
τ_{bu}	(MPa)	3.24	3.24	3.45	5.49	5.49	5.49
τ_{bu} (AIJ Guidelines)	(MPa)	3.24	3.24	3.45	3.45	3.45	3.45
$\tau_{b,exp}$	(MPa)	3.72	5.16	4.14	6.70	6.08	5.55

Failure mode* : B = bond splitting, F = flexural yield, S = shear failure

monotonic loads (specimens N2, N3, N4, N5, N6, H4 and H8) were larger than those without the hooks (specimens N1 and H0) in each test. Fig. 7 presents relationships between the shear force and the drift angle. The shear forces remained constant when the drift angle R_p exceeded 2 %. At these plateaus, the bond deterioration of flexural bars propagated, inducing splitting cracks along the bars as in Fig. 8.

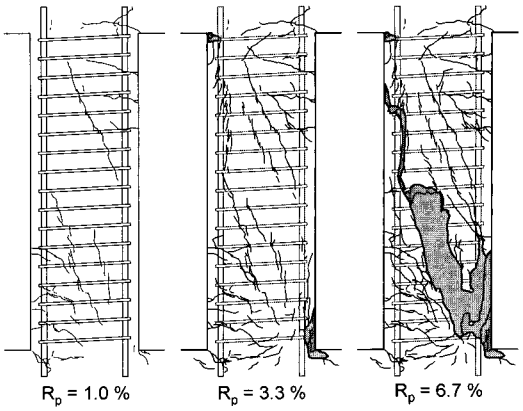

Fig. 8 Typical crack propagation (specimen H4)

The specimens under cyclic loads maintained a constant shear force after flexural yielding up to a drift angle R_p of 3 %. Specimens H6C was subjected to a larger R_p up to 5 % and resulted in a significant drop of the shear force.

4. Analysis

4.1 Bond stresses

Strains of the flexural bars measured by the strain gauges were converted into stresses using modified Ramberg-Osgood model[7]. The bond stresses were then computed by difference of the bar stresses between the adjacent strain gauges. Although the bond stresses were not equal between bars in a cross-section, they were averaged in the interest of

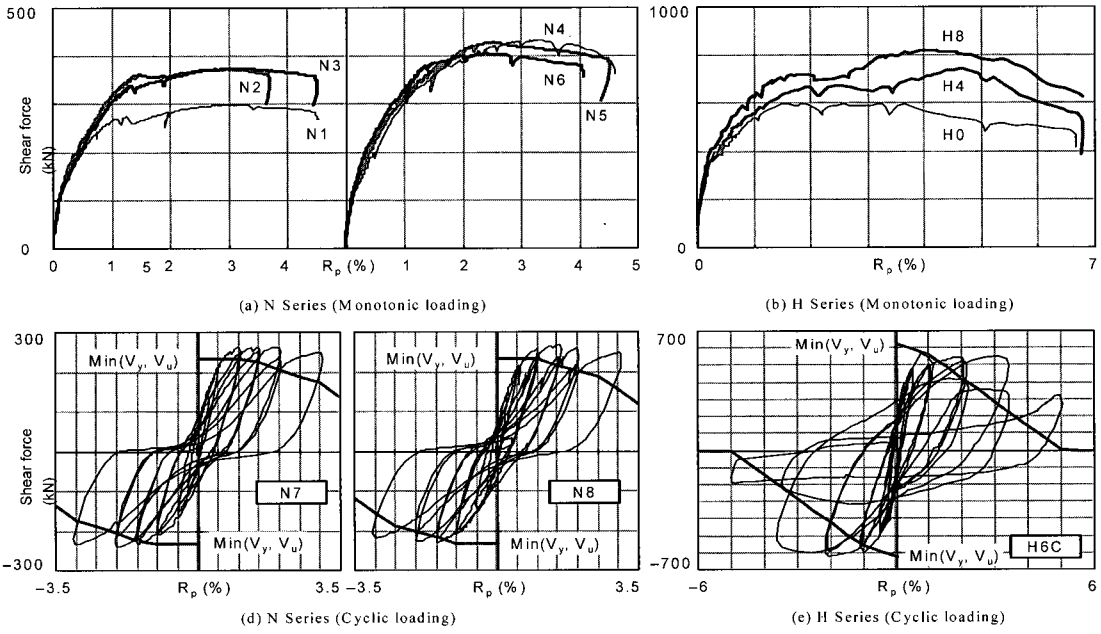

Fig. 7 Relationships between shear force and drift angle

design practice as adopted in the Guidelines[3]. Fig. 9(a) presents relationships between the averages of the bond stresses of the flexural bars and the drift angle. For the specimens under cyclic loads (N7, N8 and H6C), only the bond stresses at peak drift angle of every cycle are plotted. The maximum bond stresses are listed in Table 4.

The bond stresses remarkably increased in the specimens with the bond-strengthening hooks under monotonic loads (N2, N3, N4, N5, N6, H4 and H8) in comparison with those without the hooks (N1 and H0). The former specimens maintained the same level of the bond stresses even at a large drift angle while the latter showed descending trends of the bond stresses. Specimens under cyclic loads (N7, N8 and H6C) also presented bond deterioration at drift angle of 1.0 % or larger although the experimental bond strengths $\tau_{b,exp}$ (= maximum bond stresses) were larger than those of the specimens without the hooks.

4.2 Stresses of spirals and bond-strengthening hooks

Fig. 9(b) shows relationships between the spiral stress and the drift angle. The stresses presented in Fig. 9(b) are maximum values in the span. In all the specimens, spiral stresses exceeded 1,000 MPa and even reached the yield stress in Specimens H4 and H8. Figure 9(c) shows relationships between the bond-strengthening hook stress and the drift angle. In contrast to the spirals, the hook stresses remained lower than 300 MPa and none of them yielded. The stress-drift relations were also illustrated in Figure9(c) for the ties in Specimens N2 and N7, which had yielded.

The above observations indicated that the high-strength spirals functioned as tension-ties in a strut-tie action with a high stress over 1,000 MPa. On the other hand, the hooks improved the bond strength along longitudinal bars, but with a lower stress. The hook shall be made of inexpensive normal strength steel because the induced stress is limited by the anchorage capacity.

4.3 Bond strength

Fig. 10 shows relationships between the experimental bond strength (= maximum bond stress) and total of the reinforcement ratios of the spirals and the bond-strengthening hooks $p_w + p_b$. The bond stresses increased as the $p_w + p_b$ increased. However, the bond stress $\tau_{b,exp}$ of Specimen N6 ($p_w + p_b$ = 1.44 %) was lower than that of N8 (0.58 %), and the $\tau_{b,exp}$ of H8 (1.54 %) lower than that of

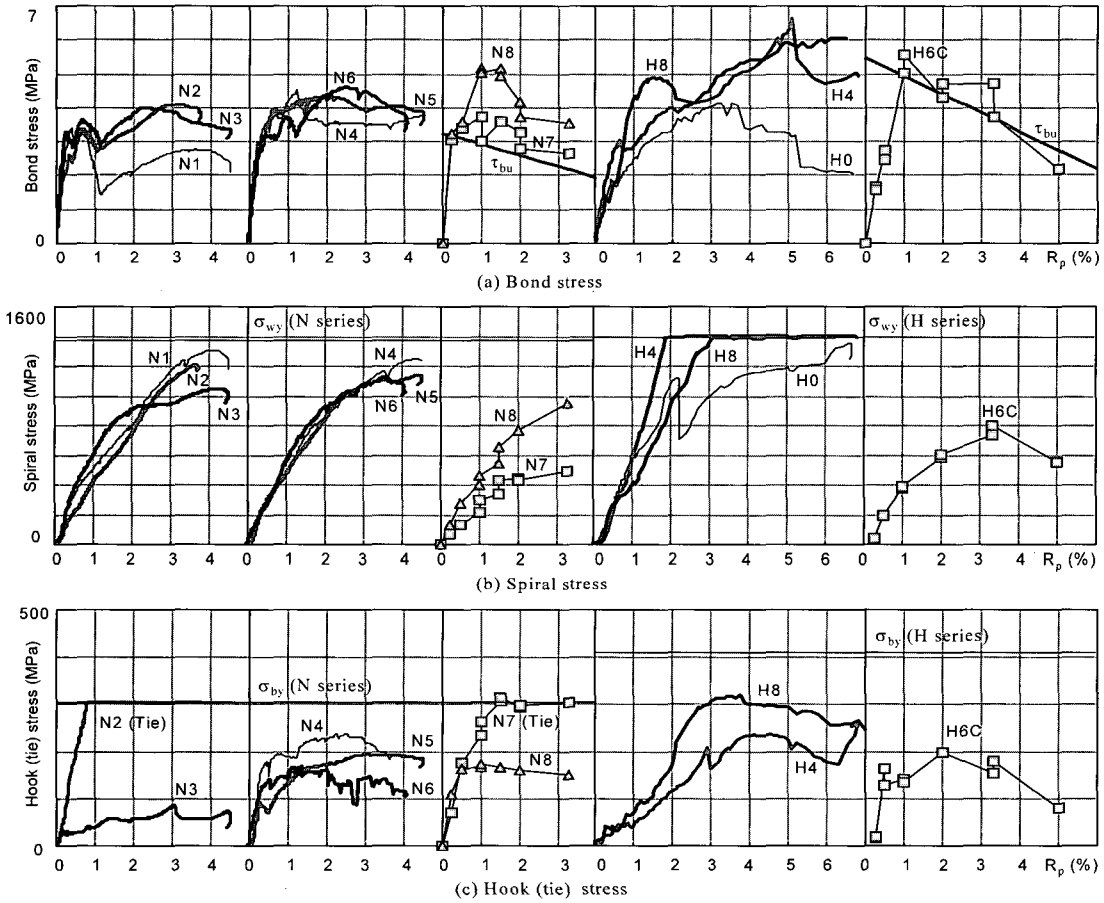

Fig. 9 Relationships between bond stress, spiral stress, hook(tie) stress and drift angle

H6C (1.29 %). This observation implies a limit of effectiveness of the bond-strengthening hooks.

The hook needs stress-transmitting zones of concrete for anchorage as illustrated in Fig. 11(a). CEB-FIP model code[4] suggests that a reinforcing bar induces stress to a concrete zone within 7(1/2) bar diameters from the reinforcement. Therefore, over-reinforcement does not increase the bond strength because it causes overlap of the adjacent stress-transmitting zones as illustrated in Fig. 11(b).

Equation (15) is to be replaced by Equation (21), which superposes contribution of the bond-strengthening hooks on that of the spirals.

$$\tau_s = \left\{54 + 45\,(N_w + N_{be}) / N_t\right\}\,(b_{si} + 1)\,(p_w + p_{be}) \quad \text{for} \quad b_{si} < b_{ci} \tag{21}$$

where,

$$p_{be} = \pi N_{be}\, d_{bb}^2 / (b_e\, s_b) \tag{22}$$

$$N_{be} = \min[N_b,\ b_e / (15\, d_{bb})\,] \tag{23}$$

Equation (21) considers only the side-splitting mode since the hook aims at prevention of the premature side-splitting failure. Equation (22) gives the effective ratio of the bond-strengthening hook p_{be}, which is determined by the effective number of the anchors N_{be}. The p_{be} represents upper limit of amount of the bond strengthening hooks. The diameter of the stress transmission zone is given by 15 times bar diameter as illustrated in Fig. 11(a). This diameter determines the N_{be} as expressed by Eq. (23). Here the N_{be} must not be integer. It should be noted that Equations (21)–(23) are available only when anchorage of the bond-strengthening hook is longer than twelve times d_{bb} [2] and inserted deeper than a quarter of the member depth (D/4). Solid lines in Figure 10 indicate the bond strengths calculated by Eqs. (11)~(14), (17) and (21)~(23). The dotted lines indicate those based on AIJ Guidelines, where the contributions of the hooks were neglected.

For specimens under cyclic loads, the bond deterioration is considered by the factor β_p defined in Equation (12). The β_p reduces the bond strength linearly with respect to the drift angle. Fig. 9(a) compares the calculated bond strengths of Specimens N7, N8 and H6C with the test results. The calculated strengths of Specimens N7 and N8 are the same. The equations provided good estimates of the descending bond stresses.

4.4 Shear strength estimation

Fig. 12 compares the experimental and the calculated shear strengths for specimens under monotonic loads. The strengths based on the proposed equations remain constant

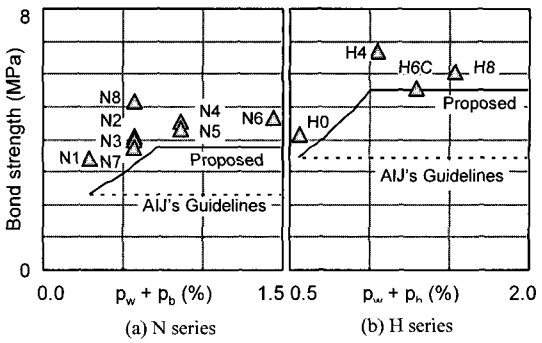

Fig. 10 *Bond strength – reinforcement ratio relations*

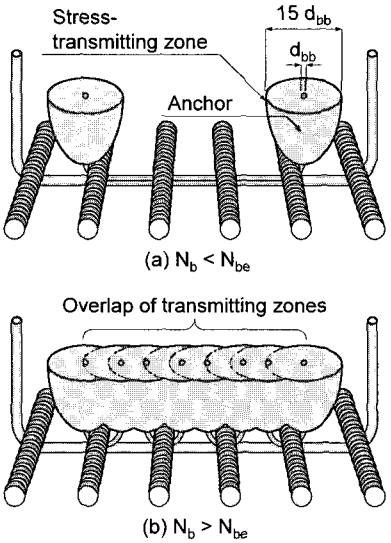

Fig. 11 Stress – transmitting zones of concrete around anchors of bond-strengthening hooks

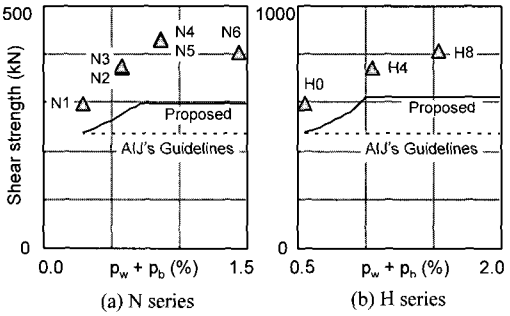

Fig. 12 Shear strength-reinforcement ratio relations for specimens under monotonic loads

at $p_w + p_b$ larger than 0.7 % for N series and 1.0 % for H series because of the upper limit of the effective reinforcement ratio p_{be} of the bond-strengthening hooks defined by Eqs. (22) and (23). The shear strength of a member under a cyclic load is limited by the flexural capacity and the bond strength. Equations (24)–(27) provide an approximate strength determined by the flexural yielding V_y [3];

$$V_y = 2M_u / L \quad (24)$$

where,

$$M_u = 0.9\, a_t\, \sigma_{ty}\, d \qquad \text{for } N = 0 \quad (25)$$

$$M_u = 0.8\, a_t\, \sigma_{ty}\, D + 0.5\, N\, D\{1 - \mathrm{N}/(bD\sigma_B)\}, \text{ for } N > 0 \quad (26)$$

$$a_t = N_t\, \pi\, d_{bt}^2 / 4 \quad (27)$$

N = compressive axial force ($N > 0$).

The calculated shear strengths for cyclic loading conditions are drawn in Fig. 7. The strengths are limited by the flexural capacity V_y in a smaller drift angle, and then begin to decrease because of the bond deterioration. These calculations provide modest estimates of the shear strengths for both the monotonic and the cyclic loading conditions.

5. Conclusions

Effectiveness of the bond-strengthening hooks was investigated through monotonic and cyclic loading tests of twelve RC specimens, which consisted of 1,300 MPa-class spirals. The anchor length of the hook l_b was twelve times the hook diameter (12 d_{bb}), and the anchors were inserted deeper than a quarter of the member depth (D/4). The following remarks were made based on the test results;

1) The proposed bond-strengthening hooks increased the bond strengths along flexural reinforcing bars and the shear strengths of members. The specimens maintained the shear strengths at least up to drift angle of 3 % even under cyclic loads.

2) Effectiveness of the bond-strengthening hook was limited because the anchor of the hook needed stress-transmitting zone of concrete. Diameter of this zone assumed to be 15times the hook diameter according to CEB-FIP model code.

This work was supported by the RRC/NMR program of MOCIE in Kongju National University and Neturen Corporation (Japan).

References

1. Sato, Y. et al., "Buckling of longitudinal bars of RC columns strengthened with continuous fiber sheet", *Proceedings of the Japan Concrete Institute*, Vol.24, No.3, 2002, pp.2036~2041.
2. AIJ, *Recommendation for Detailing and Placing of Concrete Reinforcement*, AIJ, 1986, pp.13~17.
3. AIJ, *Design Guidelines for Earthquake Resistant Reinforced Concrete Buildings Based on Inelastic Displacement Concept*, AIJ, 1999, pp.138~192.
4. CEB-FIP, *Model Code for Concrete Structures*, CEB-FIP International Recommendations, 3rd edition, Comité Euro-International du Béton, Paris, 1978, pp.155~160.
5. Kim, K. et al., "Hook-Shaped Reinforcement for Bond Splitting Prevention in RC Beams", *Summaries of Technical Papers of Annual Meeting*, AIJ, 2002 C-2, pp.289~292.
6. Sato, Y. and Fujii, S., "Local stresses and crack displacements in reinforced concrete elements", *Journal of Structural Engineering*, ASCE, Vol.128, No.10, 2002, pp. 1263~1271.
7. Vecchio, F., J., "Towards Cyclic Load Modeling of Reinforced Concrete", *ACI Structural Journal*, Vol.96, No.2, 1999, pp.193~202.